

Current-Induced Membrane Discharge

M. B. Andersen,^{1,2} M. van Soestbergen,^{3,4} A. Mani,² H. Bruus,¹ P. M. Biesheuvel,^{3,5} and M. Z. Bazant⁶

¹*Department of Micro- and Nanotechnology, Technical University of Denmark, DTU Nanotech Building 345 East, DK-2800 Kongens Lyngby, Denmark*

²*Department of Mechanical Engineering, Stanford University, Stanford, CA, 94305, USA*

³*Wetsus, Centre of Excellence for Sustainable Water Technology, Agora 1, 8934 CJ Leeuwarden, The Netherlands*

⁴*Department of Applied Physics, Eindhoven University of Technology, Den Dolech 2, 5612 AZ Eindhoven, The Netherlands*

⁵*Department of Environmental Technology, Wageningen University, Bornse Weiland 9, 6708 WG Wageningen, The Netherlands*

⁶*Departments of Chemical Engineering and Mathematics, Massachusetts Institute of Technology, Cambridge, MA, 02139, USA.*

(Dated: March 1, 2012)

Possible mechanisms for over-limiting current (OLC) through aqueous ion-exchange membranes (exceeding diffusion limitation) have been debated for half a century. Flows consistent with electro-osmotic instability (EOI) have recently been observed in microfluidic experiments, but the existing theory neglects chemical effects and remains to be quantitatively tested. Here, we show that charge regulation and water self-ionization can lead to OLC by “current-induced membrane discharge” (CIMD), even in the absence of fluid flow. Salt depletion leads to a large electric field which expels water co-ions, causing the membrane to discharge and lose its selectivity. Since salt co-ions and water ions contribute to OLC, CIMD interferes with electrodialysis (salt counter-ion removal) but could be exploited for current-assisted ion exchange and pH control. CIMD also suppresses the extended space charge that leads to EOI, so it should be reconsidered in both models and experiments on OLC.

PACS numbers: 47.57.jd, 87.16.dp, 82.45.Mp, 82.33.Ln

Selective ion transport across charged, water-filled membranes plays a major role in ion exchange and desalination [1, 2], electrophysiology [3], fuel cells [4, 5], and lab-on-a-chip devices [6–10], but is not yet fully understood. A long-standing open question has been to explain experimentally observed overlimiting current (OLC), exceeding classical diffusion limitation [11]. Possible mechanisms include electroosmotic instability (EOI) and water splitting in the bulk solution [12, 13], as well as surface conduction and electro-osmotic flow in microchannels [14]. Vortices consistent with EOI have recently been observed under OLC conditions [7, 15, 16], although the theory of Rubinstein and Zaltzman [17–19] remains to be tested quantitatively. The water splitting mechanism, either catalyzed by membrane surface groups or through the second Wien effect, has not yet been conclusively tied to OLC [13, 20–23].

In this Letter, we propose a chemical mechanism for OLC, “current-induced membrane discharge” (CIMD), resulting from membrane (de)protonation and water self-ionization, even in the absence of fluid flow. The amphoteric nature of the charge of ion-exchange membranes (i.e. sensitivity to pH and other stimuli) is well known [5, 24–29], but not the response to a large applied current. The basic physics of CIMD is illustrated in Fig. 1 for an anion-exchange membrane. During OLC, a large electric field develops on the upstream, salt-depleted side of the membrane, which expels H^+ and attracts OH^- , causing the membrane to deprotonate and lose selectiv-

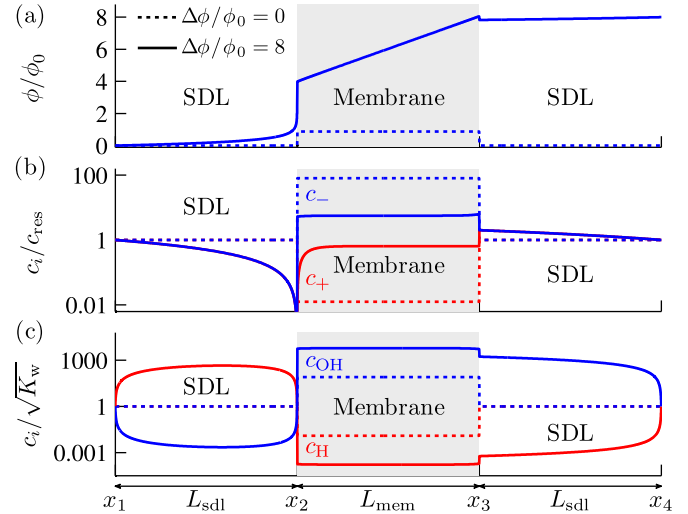
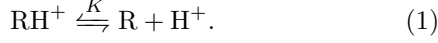


FIG. 1. [Color online] Basic physics of CIMD, illustrated by numerical solutions of Eqs. (2), (5), and (6) for an anion exchange membrane between two stagnant diffusion layers (SDL) for (a) electrostatic potential and concentrations of (b) cations c_+ and anions c_- and (c) protons c_H and hydroxyl ions c_{OH} .

ity, thereby allowing salt co-ions to pass and producing large pH gradients. The upstream solution becomes more acidic (low pH), while the downstream, salt-enriched solution and the membrane become more basic (high pH).

The local charge of an aqueous membrane strongly de-

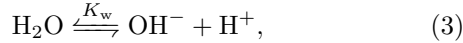
depends on the local pH. In our examples below, we consider an anion-exchange membrane with fixed surface groups of volumetric concentration c_{mem} , which selectively allows negatively charged anions (counter-ions) to pass, while blocking cations (co-ions) [30]. Depending on $\text{pH} \approx \text{p}[\text{H}] = -\log_{10}(c_{\text{H}})$, where c_{H} is the proton concentration (H^+ or H_3O^+) in M, the membrane can “discharge” (deprotonate):



The ratio of product to reactant concentrations in equilibrium is the dissociation constant K in M ($\text{p}K = -\log_{10} K$). Assuming a classical Langmuir adsorption isotherm [24–28, 31, 32], the ionization degree of the membrane,

$$\alpha = \left(1 + \frac{K}{c_{\text{H}}}\right)^{-1} = (1 + 10^{\text{pH}-\text{p}K})^{-1}, \quad (2)$$

relates its charge concentration αc_{mem} to pH and $\text{p}K$. (For a cation-exchange membrane, the power is $\text{p}K - \text{pH}$.) To describe the local pH, we cannot assume Boltzmann equilibrium with an external reservoir. Instead, we consider ion transport coupled to membrane discharge Eq. (1) and water self-ionization,



with dissociation constant

$$K_{\text{w}} = c_{\text{H}} c_{\text{OH}} \quad (4)$$

where $K_{\text{w}} = 10^{-14} \text{ M}^2$ at $T = 25^\circ\text{C}$. Although kinetics can be included [5, 20–22, 33], the reactions (1) and (3) are typically fast, so we assume local quasi-equilibrium.

We now develop a membrane model (seemingly the first) including all of these effects: (i) transport of four ionic species, including co-ions and water ions (H^+ and OH^-) along with majority anions, (ii) water self-ionization, and (iii) pH-dependent membrane charge. We consider the prototypical 1D electrodialysis geometry in Fig. 1, consisting of a planar ion-selective membrane of thickness L_{mem} between two well-stirred reservoir compartments of salt ion concentration c_{res} and pH of pH_{res} . We adopt the simplest and most commonly used model of diffusion limitation [11], in which ion concentrations vary across “stagnant diffusion layers” (SDL) of thickness L_{sdl} (of the order 10–100 μm) between the reservoirs and the membrane, e.g. representing convection-diffusion boundary layers or stagnant gel films.

Ionic diffusion, electromigration and reactions are described by four Nernst-Planck equations. Following Refs. [24, 25, 34], we combine the Nernst-Planck equations for H^+ and OH^- using Eq. (4) to eliminate the reaction terms and relate the water-ion current density J_{w} to the water-ion variable $c_{\text{w}} = (D_{\text{H}}c_{\text{H}} - D_{\text{OH}}c_{\text{OH}})/D_{\text{w}}$,

in which $D_{\text{w}} = \sqrt{D_{\text{H}}D_{\text{OH}}}$ is the geometric mean of the free H^+ and OH^- diffusivities. We thus arrive at the following set of coupled, nonlinear, differential equations to be solved in both SDLs and the membrane [34]:

$$\frac{dJ_i}{dx} = 0, \quad i = +, -, \text{w}, \quad (5a)$$

$$J_{\pm} = \mp f_{\text{r}} D_{\pm} \left(\frac{dc_{\pm}}{dx} \pm c_{\pm} \frac{d\phi}{dx} \right), \quad (5b)$$

$$J_{\text{w}} = -f_{\text{r}} D_{\text{w}} \left(\frac{dc_{\text{w}}}{dx} + [4K_{\text{w}} + c_{\text{w}}^2]^{\frac{1}{2}} \frac{d\phi}{dx} \right), \quad (5c)$$

where J_i is the ionic current density of species i and f_{r} is a hindrance factor accounting for porosity, tortuosity and constriction ($f_{\text{r}} = 1$ in the SDLs). Here, ϕ is the dimensionless mean electrostatic potential scaled to the thermal voltage $V_{\text{T}} = k_{\text{B}}T/e = 25.7 \text{ mV}$ and satisfying Poisson’s equation

$$\frac{d^2\phi}{dx^2} = -4\pi\lambda_{\text{B}} (\rho_{\text{ions}} + \rho_{\text{mem}}), \quad (6)$$

where $\lambda_{\text{B}} = e^2/(4\pi\epsilon_{\text{r},j}\epsilon_0 k_{\text{B}}T)$ is the Bjerrum length, and $\rho_{\text{ions}} = \epsilon (c_{+} - c_{-} + c_{\text{H}} - c_{\text{OH}})$ and $\rho_{\text{mem}} = \alpha \epsilon c_{\text{mem}}$ are charge densities due to the ions and the immobilized charges in the membrane, respectively. The porosity ϵ of the membrane appears because concentrations c_i are defined with respect to the interstitial, not total, volume ($\epsilon = 1$ in the SDLs). In our simulations below, we choose the following typical parameters: $c_{\text{mem}} = 5 \text{ M}$, $\text{p}K = 9.5$, $L_{\text{mem}} = L_{\text{sdl}} = 100 \mu\text{m}$, $\epsilon_{\text{r},\text{sdl}} = 78$, $\epsilon_{\text{r},\text{mem}} = 29$, $\epsilon = 0.4$, $f_{\text{r}} = 0.02$ [35], $D_{+} = 1.3 \times 10^{-9} \text{ m}^2 \text{ s}^{-1}$ and $D_{-} = 2.0 \times 10^{-9} \text{ m}^2 \text{ s}^{-1}$ (corresponding to NaCl), $D_{\text{H}} = 9.3 \times 10^{-9} \text{ m}^2 \text{ s}^{-1}$, and $D_{\text{OH}} = 5.3 \times 10^{-9} \text{ m}^2 \text{ s}^{-1}$. We also use $\text{pH}_{\text{res}} = 7$ and $\beta = 2c_{\text{res}}/c_{\text{mem}} = 0.02$, unless otherwise noted. The voltage difference across the system is $\Delta\phi$. At the reservoir/SDL boundaries we set $c_{\pm} = c_{\text{res}}$ and relate c_{w} to pH_{res} .

In spite of neglecting fluid flow, the model still predicts OLC, as shown in Fig. 1. The classical ion concentration polarization phenomenon is apparent in panel (b) with salt depletion where counter-ions (anions) enter ($x = x_2$) and enrichment where they leave ($x = x_3$). Within the membrane, however, anion depletion and cation (co-ion) enrichment reveal a significant loss of selectivity due to CIMD. At the same time, panel (c) shows large, order-of-magnitude variations in c_{H} , “mirrored” by c_{OH} in equilibrium Eq. (4), with proton enrichment (acidity) in the left SDL and proton depletion (basicity) in both the membrane and the right SDL. The existence of such pH variations has been confirmed experimentally in similar systems [36–39].

Motivated by this observation, we analyze the pH gradients perturbatively in the full CIMD model. We consider under-limiting currents, assume thin, quasi-equilibrium double layers (Donnan approximation) at the SDL/membrane interfaces, and solve the leading-order

problem for c_+ , c_- and ϕ with small perturbations in c_H and c_{OH} , valid when $(c_H - c_{OH})/(c_+ - c_-) \ll 1$. The resulting semi-analytical model (to be described in detail elsewhere) suffices to predict CIMD (variations of membrane charge with local pH) via Eq. (2). Numerical calculations show that pH and α are nearly constant across the membrane, so the water charge density is averaged between positions x_2 and x_3 (see below) to calculate the membrane charge and midplane pH [Fig. 2(b)] to be used in Eq. (2) to calculate α .

The final result for the most general model including membrane discharge, arbitrary values for pH_{res} and c_{res} , and the possibility that all diffusion coefficients are different, consists of Eq. (2) together with the set of algebraic equations below (see the Supplemental Material for details). First, we introduce the dimensionless salt flux variable $j_{salt} = (J_- - J_+ D_-/D_+)/J_{lim}$, in which $J_{lim} = -2D_-c_{res}/L_{sdl}$ is the “classical” limiting current density [11], and obtain the salt current-voltage relation,

$$\Delta\phi = 4 \tanh^{-1}(j_{salt}) + \frac{j_{salt}}{\gamma} \frac{\beta}{\alpha}, \quad (7)$$

in which $\gamma = f_r/l_{mem}$, where $l_{mem} = L_{mem}/L_{sdl}$ is the membrane-to-SDL width ratio. The first term describes concentration polarization in the SDLs, while the second is the Ohmic response of the membrane. Next, we introduce the dimensionless water ion flux $j_w = J_w L_{sdl}/(D_w \sqrt{K_w})$ and water ion variable $\rho_w = c_w/\sqrt{K_w}$ and obtain the following equations, $\rho_w(x_3^{mem}) - \rho_w(x_2^{mem}) \exp[j_{salt} \beta/(\gamma \alpha)] + j_w/\gamma = 0$, $\sinh^{-1}[\rho_w(x_i^{mem})/2] = \sinh^{-1}[\rho_w(x_i^{sdl})/2] - \sinh^{-1}(\alpha/[\beta(1 \mp j_{salt})])$, and $\rho_w(x_i^{sdl}) = \rho_w^{res} \mp j_w + \rho_0[1 + 2\gamma\beta/\alpha] \ln(1 \mp j_{salt})$, (where in these expressions $i = 2$ and 3 corresponds to $-$ and $+$, respectively). Here, ρ_w^{res} is related to pH_{res} and $\rho_0 = [4 + (\rho_w^{res})^2]^{1/2}$. Note that x_i^{mem} and x_i^{sdl} refer to positions on either side of the equilibrium electric double layer at the membrane-SDL interfaces. In the limit of an infinite membrane charge $\beta/\alpha \rightarrow 0$ the solution to the leading order problem [Eq. (7)] is simply the “classical” result [40], $j_{salt} = \tanh(\Delta\phi/4)$. We find the characteristic voltage factor ϕ_0 by expanding Eq. (7) for small $j_{salt} \ll 1$ and obtain $j_{salt} = \Delta\phi/\phi_0$ in which $\phi_0 = 4 + \beta/\gamma$ assuming constant $\alpha = 1$.

Results of the semi-analytical model are compared with full numerical calculations in Fig. 2, which shows good agreement in the expected range of validity $\Delta\phi/\phi_0 \lesssim 1$. The pH appears to converge towards a limiting value for $\Delta\phi \rightarrow \infty$, and the jump in this limiting pH-value between the left SDL and the membrane is huge, here about 5 pH units at the highest values of $\Delta\phi$ considered. We note that the deviation between the analytical and numerical solution is largest in the left SDL where electroneutrality is most strongly violated. This comparative analysis constitutes a validation of our numerics and provides further support for our conclusions

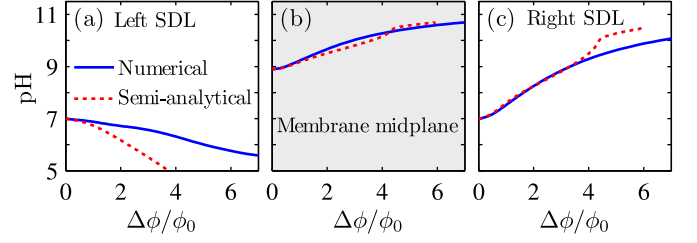


FIG. 2. [Color online] Predicted pH variations from the full numerical model, compared to the semi-analytical approximation, as a function of the applied voltage (a) in the left SDL, just next to the membrane, (b) at the membrane midplane, and (c) in the right SDL, next to the membrane.

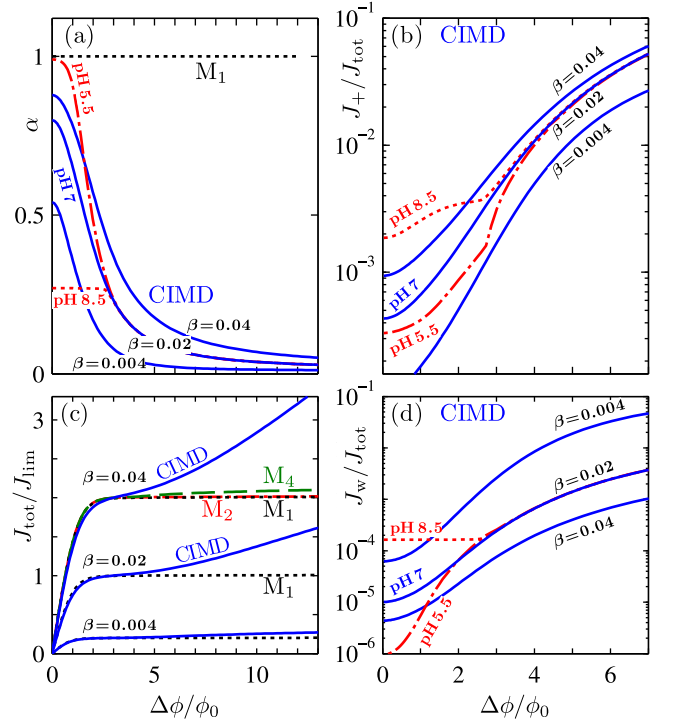


FIG. 3. [Color online] Comparison of the classical M_1 model (only counterions in the membrane) with the full CIMD model (label “pH” refers to pH_{res}). (a) Membrane ionization degree α . (b) co-ion current J_+ . (c) Total current J_{tot} . (d) Water ion current J_w .

regarding the role of pH as controlling the ionic transport properties of ion-selective membranes.

We now turn to a numerical analysis of the CIMD model Eqs. (2)–(6). For comparison, we also solve the classical model M_1 used in all prior work on EOI [15–19] in which (i) $c_- = 0$ in the membrane, (ii) $c_H = c_{OH} = 0$ everywhere, and (iii) $\alpha = 1$ for all conditions. We also solve two intermediate models which include co-ions in the membrane with $\alpha = 1$ and either *exclude* (M_2) or *include* (M_4) water ions, i.e. taking 2 or 4 ions into account in the membrane, respectively. The total current density is $J_{tot} = J_+ + J_- + J_w$.

Figure 3(a) shows the significant decrease in the ionization degree α predicted by the CIMD model, in contrast to the constant $\alpha = 1$ in the M_1 model. Moreover, α decreases with decreasing β (due to increasing Donnan potential) and decreases with pH_{res} (due to decreasing c_H in the membrane). A striking, and yet unexplained prediction is that for pH_{res} larger than 7 the ionization degree is almost constant until the curve hits that for $\text{pH}_{\text{res}} = 7$ after which the curves follow each other. In general we find beyond a few times ϕ_0 that reservoir pH has a very small influence on membrane charge, fluxes and currents (see also Fig. 3(b)-(d)). Figure 3(b) shows the significant increase of co-ion flux J_+ , thus loss of membrane selectivity, with increasing voltage, as predicted by the CIMD model, for all values of pH and β , while Fig. 3(d) shows likewise the increase in current density J_w due to water ions. Still, these contributions do not sum to the increased current during OLC, as shown in Fig. 3(c), the difference being due to increased counter-ion flux J_- .

Although the current-voltage relation in CIMD is quite complicated, our simulations and analysis suggest two general trends: (i) OLC increases with reservoir salt concentration, roughly as $\beta^{0.65}$ for the parameters of Fig. 3; (ii) OLC is nearly independent of reservoir pH, in spite of the large pH gradients produced across the membrane.

Finally, we analyze the possible effect of CIMD on EOI. In the classical M_1 model, non-equilibrium space charge forms at the limiting current [40–43], and its growing separation from the membrane reduces viscous resistance to electro-osmotic flow and destabilizes the fluid [17–19]. As a measure of the propensity to develop EOI we use the transverse (Helmholtz–Smoluchowski) electroosmotic mobility $\mu_{\text{eo}}/\mu_{\text{eo},0}$ at the left SDL-reservoir edge, which is equal to the first moment of the charge density, $-4\pi\lambda_B \int_{x_1}^{x_2} x \rho_{\text{ions}} dx$, or the dimensionless potential difference across the left SDL, $\phi(x_1) - \phi(x_2)$.

Figure 4(a) shows that slightly above the limiting current ($J_{\text{tot}}/J_{\text{lim}} = 1.01$) the M_1 model already predicts a very significant extended space charge layer (the “shoulder” maximum in $\rho_{\text{ions}}/\rho_{\text{ions},0} = (\lambda_D L_{\text{sdl}}/\phi_0) d^2\phi/dx^2$ several hundred Debye lengths from the membrane), whereas for an even higher current ($J_{\text{tot}}/J_{\text{lim}} = 1.03$), using the more realistic CIMD model, the extension of this layer is still very minor. The two intermediate models lie in between. Figure 4(b) shows how the transverse electroosmotic mobility is predicted by the M_1 model to diverge at the limiting current. This divergence is significantly reduced only by the full CIMD model including simultaneously co-ion access, water ion transport, water splitting, and membrane discharge. We note that a proper analysis of EOI would be more involved, since here we have simply focused on the transverse electroosmotic mobility as a way of illustrating the suppression of EOI due to CIMD.

In conclusion, we have theoretically demonstrated that OLC through aqueous ion-exchange membranes

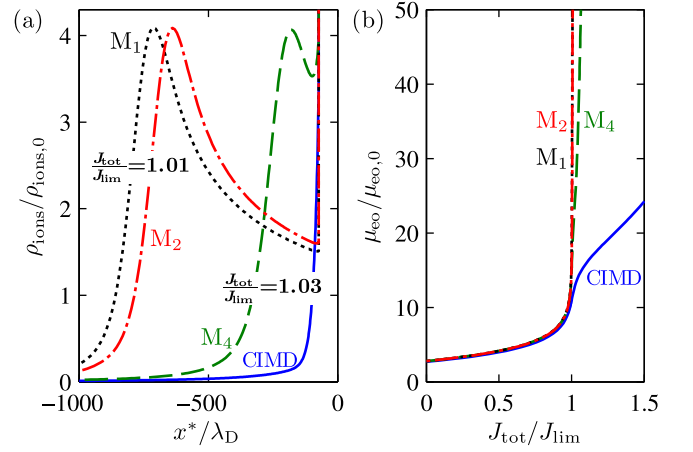


FIG. 4. [Color online] Comparison of three fixed-charge membrane models M_n having $n = 1, 2$, or 4 mobile ionic species and the CIMD model for (a) charge density ρ_{ions} versus distance x^* from the membrane scaled to the reservoir Debye length λ_D , and (b) electroosmotic mobility μ_{eo} as function of total current J_{tot} .

can result from CIMD, or loss ion selectivity due to (de-)protonation coupled to ion transport and water self-ionization. The appearance of OLC carried partially by salt co-ions and water ions reduces separation efficiency in electrodialysis, but the associated large pH gradients and membrane discharge could be exploited for current-assisted ion exchange or pH control. CIMD also suppresses the non-equilibrium space charge responsible for EOI and thus should be considered in both models and experiments on OLC with fluid flow. Although we have developed the theory for ion-exchange membranes in aqueous solutions, CIMD could occur in any nanofluidic system with an electrolyte whose ions regulate the surface charge.

-
- [1] F. G. Helfferich, *Ion exchange* (McGraw-Hill, 1962; Dover 1995).
 - [2] X. Tongwen, *J Membrane Sci* **263**, 1 (2005).
 - [3] T. F. Weiss, *Cellular Biophysics* (MIT Press, 1996).
 - [4] R. P. O'Hare, S.-W. Cha, W. G. Colella, and F. B. Prinz, *Fuel Cell Fundamentals* (Wiley, 2009).
 - [5] P. Berg, K. Promislow, J. S. Pierre, J. Stumper, and B. Wetton, *J Electrochem Soc* **151**, A341 (2004).
 - [6] Y.-C. Wang, A. L. Stevens, and J. Han, *Anal Chem* **77**, 4293 (2005).
 - [7] S. J. Kim, Y.-C. Wang, J. H. Lee, H. Jang, and J. Han, *Phys Rev Lett* **99**, 044501 (2007).
 - [8] R. Schoch, J. Han, and P. Renaud, *Rev Mod Phys* **80**, 839 (2008).
 - [9] W. Sparreboom, A. van den Berg, and J. C. T. Eijkel, *Nat Nanotechnol* **4**, 713 (2009).
 - [10] S. J. Kim, S. H. Ko, K. H. Kang, and J. Han, *Nat Nanotechnol* **5**, 297 (2010).

- [11] V. G. Levich, *Physicochemical Hydrodynamics* (Prentice-Hall, New York, 1962).
- [12] V. V. Nikonenko, N. D. Pismenskaya, E. I. Belova, P. Sibat, P. Huguet, G. Pourcelly, and C. Larchet, *Adv Colloid Interface Sci* **160**, 101 (2010).
- [13] L.-J. Cheng and H.-C. Chang, *Biomicrofluidics* **5**, 046502 (2011).
- [14] E. V. Dydek, B. Zaltzman, I. Rubinstein, D. S. Deng, A. Mani, and M. Z. Bazant, *Phys Rev Lett* **107**, 118301 (2011).
- [15] S. M. Rubinstein, G. Manukyan, A. Staicu, I. Rubinstein, B. Zaltzman, R. G. H. Lammertink, F. Mugele, and M. Wessling, *Phys Rev Lett* **101**, 236101 (2008).
- [16] G. Yossifon and H.-C. Chang, *Phys Rev Lett* **101**, 254501 (2008).
- [17] I. Rubinstein and B. Zaltzman, *Phys Rev E* **62**, 2238 (2000).
- [18] I. Rubinstein, B. Zaltzman, J. Pretz, and C. Linder, *Russ J Electrochem* **38**, 853 (2002).
- [19] B. Zaltzman and I. Rubinstein, *J Fluid Mech* **579**, 173 (2007).
- [20] R. Simons, *Nature* **280**, 824 (1979).
- [21] R. Simons, *Electrochimica Acta* **29**, 151 (1984).
- [22] C.-O. Danielsson, A. Dahlkild, A. Velin, and M. Behm, *Electrochimica Acta* **54**, 2983 (2009).
- [23] Y. Tanaka, *J Membrane Sci* **350**, 347 (2010).
- [24] P. Ramirez, A. Alcaraz, and S. Mafe, *J Electroanal Chem* **436**, 119 (1997).
- [25] P. Ramirez, S. Mafe, A. Tanioka, and K. Saito, *Polymer* **38**, 4931 (1997).
- [26] W. B. S. de Lint, P. M. Biesheuvel, and H. Verweij, *J Colloid Interface Sci* **251**, 131 (2002).
- [27] R. Takagi and M. Nakagaki, *Sep Purif Technol* **32**, 65 (2003).
- [28] S. Bandini, *J Membrane Sci* **264**, 75 (2005).
- [29] K. L. Jensen, J. T. Kristensen, A. M. Crumrine, M. B. Andersen, H. Bruus, and S. Pennathur, *Phys Rev E* **83**, 056307 (2011).
- [30] A. Yaroshchuk, *J Membrane Sci* **396**, 43 (2012).
- [31] K. Köhler, P. M. Biesheuvel, R. Weinkamer, H. Möhwald, and G. B. Sukhorukov, *Phys Rev Lett* **97**, 188301 (2006).
- [32] P. M. Biesheuvel, T. Mauser, G. B. Sukhorukov, and H. Möhwald, *Macromolecules* **39**, 8480 (2006).
- [33] P. M. Biesheuvel, *Langmuir* **18**, 5566 (2002).
- [34] M. Van Soestbergen, A. Mavinkurve, R. T. H. Rongen, K. M. B. Jansen, L. J. Ernst, and G. Q. Zhang, *Electrochimica Acta* **55**, 5459 (2010).
- [35] A. Elattar, A. Elmidaoui, N. Pismenskaia, C. Gavach, and G. Pourcelly, *J Membrane Sci* **143**, 249 (1998).
- [36] A. P. Thoma, A. Viviani-Nauer, S. Arvanitis, W. E. Morf, and W. Simon, *Anal Chem* **49**, 1567 (1977).
- [37] L. Jialin, W. Yazhen, Y. Changying, L. Guangdou, and S. Hong, *J Membrane Sci* **147**, 247 (1998).
- [38] J. J. Krol, M. Wessling, and H. Strathmann, *J Membrane Sci* **162**, 145 (1999).
- [39] J.-H. Choi, H.-J. Lee, and S.-H. Moon, *J Colloid Interface Sci* **238**, 188 (2001).
- [40] M. Z. Bazant, K. T. Chu, and B. J. Bayly, *SIAM J Appl Math* **65**, 1463 (2005).
- [41] I. Rubinstein and L. Shtilman, *J Chem Soc, Faraday Trans 2* **75**, 231 (1979).
- [42] K. T. Chu and M. Z. Bazant, *SIAM J Appl Math* **65**, 1485 (2005).
- [43] P. M. Biesheuvel, M. van Soestbergen, and M. Z. Bazant, *Electrochimica Acta* **54**, 4857 (2009).